Rotational Reorientation Dynamics of Nonlinear Optical Chromophores in Rubbery and Glassy Polymers: α-Relaxation Dynamics Probed by Second Harmonic Generation and Dielectric Relaxation

Ali Dhinojwala,† George K. Wong,‡ and John M. Torkelson*,†,§

Department of Chemical Engineering, Department of Physics and Astronomy, and Department of Materials Science and Engineering, Northwestern University, Evanston, Illinois 60208-3120

Received February 22, 1993; Revised Manuscript Received July 26, 1993•

ABSTRACT: Second harmonic generation (SHG) is used to monitor rotational, reorientation dynamics of disperse red 1 (DR1) doped at 2 wt % in poly(isobutyl methacrylate) (PIBMA) and poly(ethyl methacrylate) (PEMA). A delay-trigger approach is employed in conjunction with conventional measurements to monitor dynamics from 10^{-4} s to as long as necessary, permitting characterization of rotational reorientation above and below T_g. The dynamics of the orientation component of the second-order macroscopic susceptibility, $\chi^{(2)}$, is shown to be sensitive to $\langle\cos\theta\rangle$, where θ is the angle between the direction vector of the applied dc field and that of the chromophore dipole moment. Both in poling-onset-mode and temporal decay experiments, the time dependence of the orientational component of $\chi^{(2)}$ can be represented by a Kohlrausch–Williams–Watts equation, from which average rotational reorientation time constants, $\langle\tau\rangle$, may be determined. By comparison of SHG and dielectric relaxation measurements in PIBMA, which exhibits only an α-relaxation, and PEMA, which exhibits distinct α- and β-relaxations at temperatures $T \leq 1.15$–$1.17T_g$, the rotational, reorientation dynamics of DR1 are shown to be coupled with the α-relaxation dynamics in these polymers. $\langle\tau\rangle$ values are obtained over a seven decade range and fit well to WLF equations above T_g but deviate below T_g; scaling the $\langle\tau\rangle$ data using the reduced variable T_g/T reveals good overlap for the two polymers, indicating similarity in the cooperativity of the α-relaxations in PIBMA and PEMA. The implications of the coupling of nonlinear optical dopant reorientation to the polymer α-relaxation for the design of temporally stable SHG polymeric materials are discussed.

Introduction

The study of polymers for second harmonic generation (SHG), the conversion of light of frequency ω to 2ω, is over a decade old.[1-3] The interest in using polymers for second-order nonlinear optics (NLO) is related to the production of inexpensive alternatives to inorganic crystals for frequency doubling in laser and optical data storage applications and for electro-optic devices.[4-6] A major stumbling block in the application of polymers for SHG has been the temporal decay[7] of the second-order macroscopic susceptibility, $\chi^{(2)}$, related to the square root of SHG intensity; this temporal decay is evident in glassy thermoplastics and thermosets containing doped[7,8] or covalently attached[9-14] NLO chromophores. In order to obtain SHG properties in an amorphous polymer, it is necessary to make the polymeric system noncentrosymmetric by applying a poling field, resulting in a net orientation of NLO chromophore dipoles.[1] However, upon removal of the poling field, randomization of NLO chromophore orientation occurs over time,[7] resulting in a decrease in $\chi^{(2)}$ and SHG intensity.

The basis for the randomization of chromophore orientation has been the subject of significant inquiry. Several studies[7,15-17] have indicated qualitatively that the decay in $\chi^{(2)}$ is associated with glassy polymer relaxations while others[18,19] have postulated the presence of different effects, but few details have been provided. Recently, we developed a new protocol[20] (partly based on ref 21) for SHG measurement in which the laser pulse is triggered from 200 μs to 0.5 s after switching the dc-poling field on (onset measurement) or off (decay measurement); when used in conjunction with normal time-domain measurements, dynamics can be monitored over almost 10 orders of magnitude in time. Given that both rubbery and glassy polymer dynamics occur over a very broad range of time scales, our approach provides significant advantages over previous SHG studies in accurately describing the rotational dynamics of the NLO chromophores and comparing the dynamics to those of the polymer matrix.

In the present work, a direct comparison of SHG decay dynamics to the α- and β-transition dynamics of polymers can be achieved by a combination of SHG and dielectric relaxation measurements on NLO-chromophore-doped poly(isobutyl methacrylate) (PIBMA) and poly(ethyl methacrylate) (PEMA). For the polymers and chromophores, disperse red 1 (DR1) and 4-(dimethylamino)-4′-nitrostilbene (DANS), discussed here, it will be shown that the chromophore rotational, reorientation dynamics are directly coupled to the polymer α-relaxation dynamics associated with the glass transition. The implications of this coupling in the design of temporally stable second-order NLO polymers are important from several standpoints. Technologically, the necessity of using a polymer with a T_g high in comparison to use temperature will be explained in terms of the temperature dependence of the average rotational, reorientation relaxation time, $\langle\tau\rangle$, in the glassy state. Scientifically, the approaches described here demonstrate how SHG can be used as a new technique to examine quantitatively and in detail the α-transition dynamics of polymeric systems over a very broad dynamic range. While a variety of approaches, including photon correlation spectroscopy,[22-24] dielectric,[25-28] mechanical,[29,30] NMR,[31,32] fluorescence anisotropy decay,[33-35] excimer probe fluorescence,[36,37] and singlet and triplet

* To whom correspondence should be addressed.
† Department of Chemical Engineering.
‡ Department of Physics and Astronomy.
§ Department of Materials Science and Engineering.
• Abstract published in *Advance ACS Abstracts*, October 1, 1993.

0024-9297/93/2226-5943$04.00/0

transient grating[38] along with photobleaching[39,40] have been used to investigate polymer dynamics, many of the studies have been limited to a small regime of polymer behavior. In contrast, the SHG approach potentially will allow the study of polymer dynamics over a several hundred degree range in temperature.

Second Harmonic Generation Applied to Polymer Dynamics Investigations

Given that SHG experiments have only very recently been modified[20] to allow subsecond measurement of the temporal decay or onset of SHG intensity, relatively little attention has been given to the SHG technique by polymer physicists. Here we provide a brief background explaining how SHG measurables can be used to determine quantitatively the temperature and polymer dependencies of the NLO-chromophore average rotational, reorientation relaxation time constant. In turn, we indicate how chromophore rotational, reorientation dynamics may be correlated to polymer dynamics. (For a more general treatment of nonlinear optics, see refs 41–44.)

In the presence of two optical fields and a static dc field the molecular polarization at frequency 2ω is given by[45]

$$p_i(2\omega) = \beta_{ijk}(f^{\omega}E^{\omega}_j)(f^{\omega}E^{\omega}_k) + \gamma_{ijkl}(f^{\omega}E^{\omega}_j)(f^{\omega}E^{\omega}_k)(f^0E^0_l) \quad (1)$$

where i, j, k, and l refer to the molecular coordinate system, γ_{ijkl} is the molecular third-order nonlinear hyperpolarizability, E^{ω} is the optical field at frequency ω, E^0_l is the applied dc field, and $f^{\omega}(f^0)$ is the local field factor at frequency ω (0). Since SHG measurements are done on macroscopic samples that consist of many individual molecules, the macroscopic polarization at frequency 2ω can be written as

$$P_I^{2\omega} = \chi^{(2)}_{IJK}E^{\omega}_J E^{\omega}_K \quad (2)$$

where I, J, and K are the lab axes and $\chi^{(2)}_{IJK}$ is the second-order macroscopic susceptibility. For the chromophores employed in this study there is one predominant molecular tensor component, β_{333}, where 3 is the direction of the dipole moment.[46]

If θ is the angle between the applied dc field and the dipole moment, μ, then the microscopic susceptibility is related to the macroscopic susceptibility,[18] $\chi^{(2)}$, by

$$\chi^{(2)}_{zzz} = N(f_z^{\omega})^2 f_z^{2\omega}[\beta_{333}\langle\cos^3\theta\rangle + \gamma_{3333}f_z^0E_z^0\langle\cos^4\theta\rangle] \quad (3)$$

$$\chi^{(2)}_{zxx} = \frac{N(f_x^{\omega})^2 f_z^{2\omega}}{2}[\beta_{333}(\langle\cos\theta\rangle - \langle\cos^3\theta\rangle) + \gamma_{3333}f_z^0E_z^0\langle\cos^2\theta\sin^2\theta\rangle] \quad (4)$$

where N is the number density of chromophores, f_i is the local field factor in direction i, and z is the direction of the applied dc field, E_z^0. Assuming that the angular distribution of the dipole orientation is described by the Boltzmann formula, then

$$\langle\cos^{(a)}\theta\rangle = \frac{\int_0^{\pi}\exp\left\{\frac{\mu E_z^0 f_z^0\cos\theta}{kT}\right\}\cos^{(a)}\theta\sin\theta\,d\theta}{\int_0^{\pi}\exp\left\{\frac{\mu E_z^0 f_z^0\cos\theta}{kT}\right\}\sin\theta\,d\theta} \quad (5)$$

where k is the Boltzmann constant and T is absolute temperature. Using eq 5 and the approximation that the dc field is small ($\mu E_z^0 f_z^0/kT \ll 1$), eqs 3 and 4 can be written as

$$\chi^{(2)}_{zzz} = NE_z^0(f_z^{\omega})^2 f_z^{2\omega}f_z^0\left[\frac{\mu\beta_{333}}{5kT} + \gamma\right] \quad (6)$$

$$\chi^{(2)}_{zxx} = NE_z^0(f_x^{\omega})^2 f_z^{2\omega}f_z^0\left[\frac{\mu\beta_{333}}{15kT} + \frac{\gamma}{3}\right] \quad (7)$$

where $\gamma = \gamma_{3333}/5$. During experiments the SHG intensity is measured, which is related to the macroscopic susceptibility[18] by the following:

$$I_{zz}^{2\omega} \propto |\chi^{(2)}_{zzz}|^2 \quad (8a)$$

$$I_{zx}^{2\omega} \propto |\chi^{(2)}_{zxx}|^2 \quad (8b)$$

where I_{zz} is the SHG intensity polarized in the z direction generated by the incident light polarized in the z direction and I_{zx} is the SHG intensity polarized in the z direction generated by the incident light polarized in the x direction.

The first terms in brackets in eqs 6 and 7, $\mu\beta_{333}/5kT$ and $\mu\beta_{333}/15kT$, respectively, are due to the orientation of the chromophores; the second terms in brackets in eqs 6 and 7, γ and $\gamma/3$, respectively, are due to the electric-field-induced third-order effect. For all practical purposes, this latter effect appears instantaneously upon application of the dc field and disappears instantaneously upon its removal.[47] γ is usually smaller than $\mu\beta_{333}/5kT$, is difficult to measure, and in most past studies has been neglected. However, in demonstrating a quantitative relationship between the temporal decay of the SHG quantity $\chi^{(2)}$, and thereby chromophore orientation, to polymer dynamics, it is necessary to account for γ. We recently reported a method,[48] using the delay-trigger technique described in the Experimental Section, which can determine the relative contribution of γ to the overall value of $\chi^{(2)}$. This relative contribution depends on the chromophore used, not on the polymer in which it may be doped; limited studies[48,49] with several chromophores reveal that the relative contribution of γ can account for as much as 20% of $\chi^{(2)}$ in the presence of the dc field.

Once the orientation component of $\chi^{(2)}$ has been determined by appropriately subtracting out the relative contribution of γ, the temporal decay of $\chi^{(2)}$ at a given temperature can be related to any of a variety of models or theories proposed to explain the non-single-exponential relaxation behavior of amorphous polymer systems. We have used the Kohlrausch–Williams–Watts (KWW) equation[50] to model the dynamics:

$$y = \exp\left(-\left(\frac{t}{\tau}\right)^{\beta_w}\right) \quad (9)$$

where y is the relaxation parameter of interest, in this case the normalized orientation component of $\chi^{(2)}$, and τ and β_w are KWW parameters. β_w can take values between 0 and 1; $\beta_w = 1$ corresponds to a single-exponential relaxation process while $\beta_w < 1$ indicates a distribution of relaxation times.[51] The KWW equation has been chosen in this study for several reasons. First, it has been extensively used to model dielectric relaxation in amorphous polymers and supercooled liquids,[52] enthalpy,[53] quasi-elastic light scattering from ionic glasses and polymers melts,[22–24] volume relaxation in amorphous polymers,[54] NMR relaxation,[55] etc. Secondly, the quality of the present SHG data does not justify using a more complicated expression for the relaxation behavior. The use of the KWW expression is sufficient for the present

purpose of demonstrating a quantitative relationship between polymer segment dynamics and the temporal decay or onset of $\chi^{(2)}$. (More detailed and exacting studies may allow for the most appropriate relaxation relationship to be distinguished;[56] this will be the subject of future study.) If a SHG polymeric system exhibits a relaxation of the orientation component of $\chi^{(2)}$ which may be fit adequately to eq 9 at a variety of temperatures, then a comparison of polymer dynamics to the decay of $\chi^{(2)}$ may be achieved by defining an average rotational, reorientation relaxation time constant, $\langle\tau\rangle$:

$$\langle\tau\rangle = \int_0^\infty \exp\left(-\left(\frac{t}{\tau}\right)^{\beta_w}\right) dt = \frac{\tau\Gamma\left(\frac{1}{\beta_w}\right)}{\beta_w} \qquad (10)$$

where Γ is the gamma function. This approach of defining $\langle\tau\rangle$ is similar to that used in a variety of polymer dynamics studies, including those using light scattering[22-24] and dielectric relaxation.[57]

By determining the temperature and polymer dependencies of $\langle\tau\rangle$, describing the average rotational, reorientation relaxation times for NLO chromophores doped in polymers, a direct comparison may be drawn to polymer dynamics. For example, in the rubbery state ($T_g < T < T_g + 100$ °C), polymer segment dynamics associated with the α-relaxation follow the Williams–Landel–Ferry (WLF) equation.[58] If a simple correlation exists between $\langle\tau\rangle$ and the α-relaxation processes in the rubbery state, then

$$\log\left(\frac{\langle\tau\rangle}{\langle\tau\rangle_{T_g}}\right) = \frac{-C_1(T - T_g)}{C_2 + T - T_g} \qquad (11)$$

where C_1 and C_2 are WLF parameters, and $\langle\tau\rangle_{T_g}$ is the average rotational relaxation time at T_g. Besides the α-relaxation which is associated with a cooperative motion of a number of segments along the chain backbone,[29] some polymers also exhibit a β-relaxation often associated with restricted motion of a side group. If a correlation exists between $\langle\tau\rangle$ and the β-relaxation processes, then one should see an Arrhenius temperature dependence of $\langle\tau\rangle$ both above and below T_g.

If an average chromophore rotational, reorientation relaxation time can be accurately defined, then the final issue of importance is whether the reorientation dynamics depend on the tensor component of $\chi^{(2)}$ being measured, i.e., $\chi^{(2)}_{zzz}$ vs $\chi^{(2)}_{zxx}$. This issue has been addressed in a recent theoretical study by Wu.[59] Wu indicated from his solution of the transient diffusion equation based on a simple model proposed originally by Debye[60] (for freely floating dipoles in a viscous medium) that both $\chi^{(2)}_{zzz}$ and $\chi^{(2)}_{zxx}$ should show similar transient dynamics. A comparison of eqs 3 and 4[18,41] may at first seem to be in conflict with Wu's conclusion in that the orientation component of $\chi^{(2)}_{zzz}$ is seen to depend on $\langle\cos^3\theta\rangle$ while that of $\chi^{(2)}_{zxx}$ is dependent on a combination of $\langle\cos\theta\rangle$ and $\langle\cos^3\theta\rangle$. However, $\langle\cos^3\theta\rangle$ may be expressed as

$$\langle\cos^3\theta\rangle = \frac{2}{5}\langle P_3(\cos\theta)\rangle + \frac{3}{5}\langle P_1(\cos\theta)\rangle \qquad (12)$$

where P_1 and P_3 are the first and third Legendre polynomials, respectively. Equation 12 suggests that the orientation components of $\chi^{(2)}_{zzz}$ and $\chi^{(2)}_{zxx}$ will exhibit temporal decays upon removal of a dc field with two characteristic time constants, τ_1 associated with P_1 and τ_3 associated with P_3, with the time constant $\tau_n = (n(n+1)D)^{-1}$, where D is the rotational diffusion coefficient for the decay. However, according to Wu's prediction for low dc fields, the amplitude associated with τ_3, the fast decay, is very much smaller than that associated with τ_1. Thus, within experimental error the decays of the orientation components of $\chi^{(2)}_{zzz}$ and $\chi^{(2)}_{zxx}$ are predicted to be identical with a decay time of $\tau_1 = (2D)^{-1}$. The same conclusions can be reached about the onset of the orientation components of $\chi^{(2)}_{zzz}$ and $\chi^{(2)}_{zxx}$. This indicates that both the decay and onset processes described by Wu are dominated by $\langle\cos\theta\rangle$ even though eq 3 states that $\chi^{(2)}_{zzz}$ is related linearly to $\langle\cos^3\theta\rangle$ while eq 4 states $\chi^{(2)}_{zxx}$ is related linearly to a combination of $\langle\cos^3\theta\rangle$ and $\langle\cos\theta\rangle$.

If Wu's theory is applicable, it may be concluded that $\chi^{(2)}_{zzz}$ and $\chi^{(2)}_{zxx}$ should exhibit the same dynamics, with an average rotational relaxation constant $\langle\tau\rangle$ describing the decay and onset for both quantities. In section A of the Results and Discussion, the similarity in decay and onset dynamics for $\chi^{(2)}_{zzz}$ and $\chi^{(2)}_{zxx}$ is demonstrated, showing that the relaxation processes measured by SHG are independent of the tensor component of $\chi^{(2)}$ being measured, as suggested by Wu's theory. In sections B and C of the Results and Discussion, SHG relaxation dynamics are compared quantitatively to polymer dynamics of two polymer systems demonstrating that NLO chromophore reorientation dynamics are coupled to the α-transition dynamics of the polymers tested. It is also demonstrated how dielectric relaxation measurements (known to be sensitive to $\langle\cos\theta\rangle$[60]) on NLO-chromophore-doped polymers, where the dielectric relaxation is predominantly associated with the mobility of ester side groups of the polymers under study, may be compared to the SHG relaxation measurements.

Experimental Section

(A) Sample Preparation. Poly(isobutyl methacrylate) (PIBMA; M_w = 300 000, M_n = 140 000) and poly(ethyl methacrylate) (PEMA; M_w = 340 000, M_n = 126 000) were obtained from Scientific Polymer Products. Disperse red 1 (DR1; Aldrich) was recrystallized using toluene. For SHG studies, polymer + 2 wt % DR1 was dissolved in spectroscopic grade chloroform and spin coated onto a quartz substrate which was patterned with planar chrome electrodes using standard photolithographic techniques. The gap between the two chrome electrodes was 800 μm.[61] The films were dried below T_g for 24 h and above T_g for 12 h under vacuum. The final film thicknesses were 5–10 μm. The T_g's of the doped films were 61 and 53 °C for PEMA and PIBMA, respectively, while those of the homopolymer for PEMA and PIBMA were 64 and 57 °C, respectively. T_g's were measured as the onset temperature of the heat capacity change with a Perkin-Elmer DSC-7 at a heating rate of 10 °C/min. Samples for dielectric relaxation were prepared by spin coating polymer + dye onto a glass substrate sputtered with a gold layer. The films were dried below T_g for 24 h and above T_g for 12 h under vacuum. After drying, another gold layer was sputtered on top of the polymer film.

(B) Experimental Technique–SHG. SHG measurements employed a Q-switched Nd-YAG laser (10-Hz frequency) with a 1.064-μm fundamental beam. SHG intensities were obtained relative to quartz. A schematic of the instrumentation is provided in ref 7b. The rotational dynamics can be monitored by recording the SHG intensity either upon application of a dc field (poling-onset mode) or removal of a dc field (decay mode).

(i) Poling-Onset-Mode Measurements. The thermal history of the polymer film doped with the chromophore is removed first by heating the sample above T_g followed by cooling it quickly to the temperature where the measurement is to be done. In order to monitor dynamics from 200 μs to 0.5 s, a new delay-trigger approach was used (partly based on information in ref 21) as shown in Figure 1a. The laser is triggered with a 10-Hz frequency, as indicated by numbers 1–9 in Figure 1a. In order to monitor the second-order macroscopic susceptibility, $\chi^{(2)}$, at a given time, e.g. 50 ms, after application of the dc-poling field, the dc field ($V \approx 2500$ V across an 800-μm gap) is switched on 50 ms before the second laser pulse scans the sample. (The dc field used in

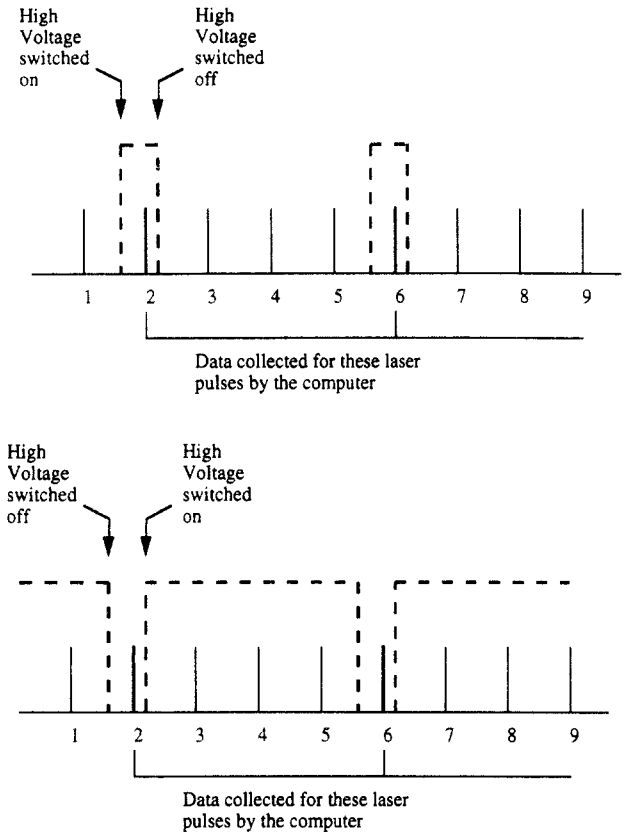

Figure 1. (a) Poling-onset-mode technique to monitor SHG transient dynamics from 10^{-4} to 0.5 s. (b) Delay-trigger technique to monitor SHG transient dynamics from 10^{-4} to 0.5 s. Refer to the text for further details.

this study is 1–2 orders of magnitude less than those used in many other SHG studies, where the goal is often to achieve large $\chi^{(2)}$ values.[7,9,11]) Afterward, the dc field is switched off again for a period greater than 5 times the period during which the dc field was applied. This was done to ensure that $\chi^{(2)}$ returned to zero before repeating the measurement. As the boxcar integrator used in these measurements collects data from the photomultiplier tube for all laser pulses, a gate was employed before the computer interface allowing only laser pulses 2, 6, etc. to be collected. One hundred pulses were collected for each decay time accessed in order to optimize the signal-to-noise ratio.

The lower limit of 200 μs for the data acquisition was due to the limitation of the high voltage power supply used in this study since the rise and fall times of the high voltage pulse were slightly less than 30 μs.[62] The higher limit of 0.5 s was chosen for expedience, as the 0.5 s measurement required approximately 6 min to achieve when all 100 repetitions of the measurement were included. It should be noted that a 1–2% error exists in our relative $\chi^{(2)}$ measurements as the high voltage supply employed here was switchable from 2500 V to ≈25 V; the latter quantity was used as an approximation of complete removal of the field (0 V). The measurements from 20 s onwards were done by switching on the the dc field permanently and averaging 100 laser pulses to achieve a high signal-to-noise ratio. Thus by using the delay trigger in combination with the conventional poling approach, we can monitor rotational dynamics over a broad range of time from 10^{-4} to potentially 10^6 s.

(ii) Decay-Mode Measurements. Ideally, decay-mode studies are to be done isothermally by applying a dc-poling field until the SHG intensity (or equivalently the NLO-chromophore orientation) reaches steady state and then removing the dc field and monitoring the temporal decay of SHG intensity (chromophore disorientation). However, achieving a steady-state SHG signal below T_g requires much time, as long as several days at T_g − 30 °C. In order to reduce the time required to reach steady state, the following procedure is employed. The sample is heated above T_g, and a dc-poling field is applied until steady state is achieved; with the dc field applied, the sample is then quenched

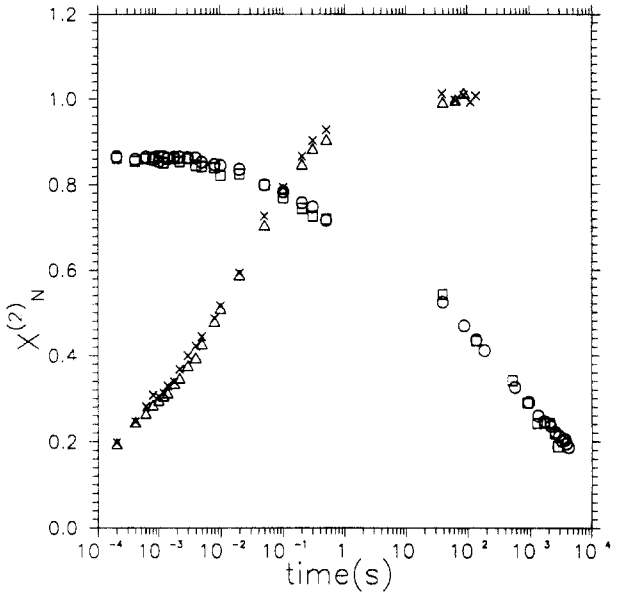

Figure 2. Comparison of rotational dynamics using SHG in PEMA + 2 wt % DR1 with decay at 40 °C ($\chi^{(2)}_{zzz}$ (○), $\chi^{(2)}_{zxx}$ (□)) and poling-onset at 74 °C ($\chi^{(2)}_{zzz}$ (△), $\chi^{(2)}_{zxx}$ (×)). $\chi^{(2)}_N$ is the susceptibility normalized with respect to the value at $t = 0$ before switching off the dc-poling field.

to the temperature at which the decay measurements are to be done. The dipole orientation after quenching with the dc field on is assumed to have reached the steady-state orientation at that temperature since no further increase in the SHG intensity is observed.

The poling conditions used in this study were 80 °C for 10–15 min for PIBMA + DR1 systems and 73 °C for 5 min for PEMA + DR1 systems. The decay-mode measurement from 200 μs to 0.5 s is done using the delay-trigger approach as shown in Figure 1b. Figure 1b is similar to Figure 1a except that the dc field is switched "off" instead of "on" and vice versa. The measurement from 20 s onward was done by switching off the dc field permanently and averaging 100 pulses to achieve a high signal-to-noise ratio. Similar to the poling-onset mode, we can use the combined approaches to monitor dynamics over eight to ten decades in time.

(C) Experimental Technique–Dielectric Relaxation. After heating the polymer + dye to the test temperature, dielectric relaxation was measured from 5 to 10^6 Hz using a Hewlett Packard 4192A impedance analyzer.

Results and Discussion

(A) Comparison of $\chi^{(2)}_{zzz}$ and $\chi^{(2)}_{zxx}$. One of the predictions of Wu's analysis[59] of the rotational dynamics of noninteracting NLO chromophores freely floating in a viscous liquid is that, within experimental error, the dynamics for both onset and decay of $\chi^{(2)}_{zzz}$ and $\chi^{(2)}_{zxx}$ are identical and thus depend only on $\langle\cos\theta\rangle$ (or the first Legendre polynomial of $\langle\cos\theta\rangle$). An important reason for determining whether the onset and decay of $\chi^{(2)}_{zzz}$ and $\chi^{(2)}_{zxx}$ are identical for systems under investigation here, i.e., NLO chromophores doped into rubbery or glassy polymers, is that a direct comparison of dielectric relaxation, dependent on $\langle\cos\theta\rangle$,[60] to SHG relaxation is then justified. Under circumstances in which the measured dielectric relaxation is associated with the polymer α (β) transition dynamics, it is then possible to determine whether SHG relaxation, and thereby the relaxation of NLO-chromophore orientation, is related to that of the α (β) transition. Such a circumstance is obtained in the dielectric relaxation of PIBMA[26] (PEMA[26]).

Figure 2 compares $\chi^{(2)}_{zzz}$ and $\chi^{(2)}_{zxx}$ for a PEMA + 2 wt % DR1 system. The decay and onset-mode measurements followed the protocol described in the Experimental

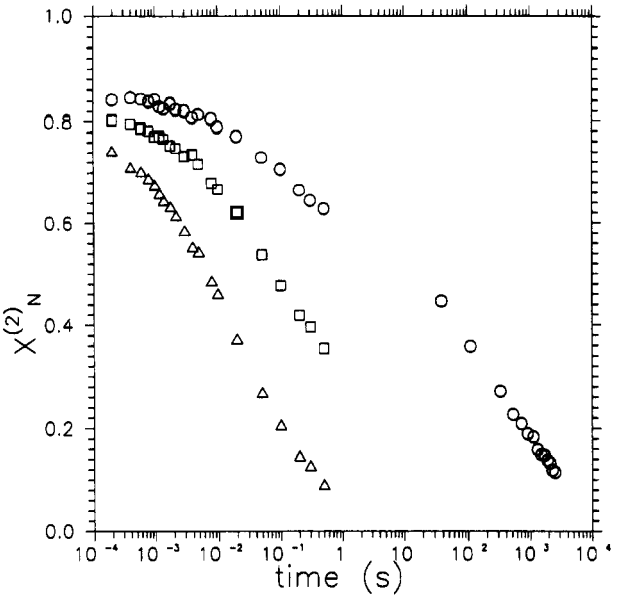

Figure 3. Decay data in PIBMA + 2 wt % DR1 at 40 (○), 58 (□), and 69 °C (△). $\chi^{(2)}_N$ is the susceptibility normalized with respect to the value at $t = 0$ before switching off the dc-poling field [$\chi^{(2)}_{zzz}/\chi^{(2)}_{zzz}(t=0)$].

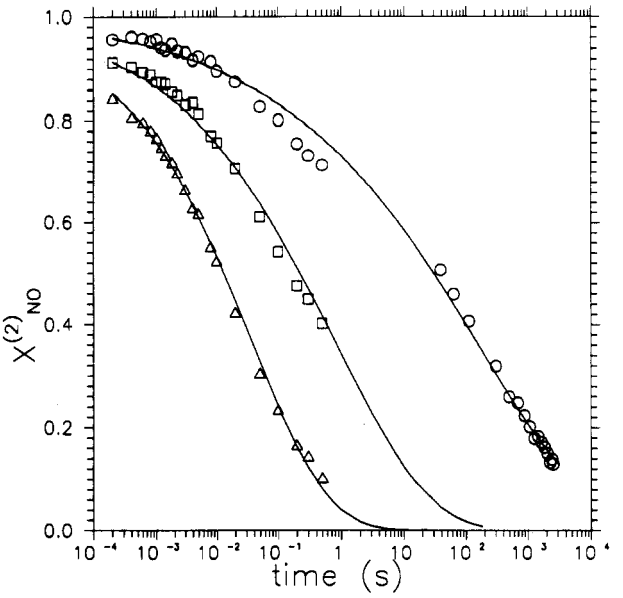

Figure 4. Decay data in PIBMA + 2 wt % DR1 at 40 (○), 58 (□), and 69 °C (△). $\chi^{(2)}_{NO}$ is the orientation component of $\chi^{(2)}_N$. (Figure 3 data corrected for the electric-field-induced third-order effect.) ($\chi^{(2)}_{NO} = \chi^{(2)}_{zzz}/(0.88\chi^{(2)}_{zzz}(t=0))$ for decay-mode data.) The solid curves are fits to the KWW equation.

Section. The decay data were taken in the glassy state at 40 °C, while the onset data were taken in the rubbery state at 74 °C. In both cases, the data in Figure 2 are shown as $\chi^{(2)}_N$ which represents the ratio of $\chi^{(2)}$ (for *zzz* or *zxx*) normalized to that measured just before switching off the dc field, in the case of decay-mode data, or that at steady state, in the case of onset-mode data. Figure 2 indicates that $\chi^{(2)}_{zzz}$ and $\chi^{(2)}_{zxx}$ dynamics are identical within experimental error regardless of whether the data are taken in decay or onset mode or whether the polymers are in the rubbery or glassy state. Also of importance is the fact that at all times $\chi^{(2)}_{zzz}/\chi^{(2)}_{zxx} = 3.0$, as predicted by eqs 6 and 7. This is a strong indication of the validity of Boltzmann statistics (eq 5) in describing the distribution of chromophore orientation in these systems.

The identical nature of the dynamics associated with $\chi^{(2)}_{zzz}$ and $\chi^{(2)}_{zxx}$ in the rubbery and glassy states demonstrates excellent agreement with the analysis by Wu[59] for the simple system of noninteracting dipoles floating freely in a viscous fluid. Given the identical nature of $\chi^{(2)}_{zzz}$ and $\chi^{(2)}_{zxx}$ dynamics in both the onset- and decay-mode measurements, in parts B and C below all the SHG data are for measurements of the *zzz* tensor only. (For simplicity, $\chi^{(2)}_{zzz}$ will be abbreviated as $\chi^{(2)}$.)

(B) Temperature Dependence in PIBMA. Figure 3 shows the SHG decay-mode measurements for the PIBMA + 2 wt % DR1 system at 40, 58, and 69 °C. The decay-mode data are represented as $\chi^{(2)}_N$, which is $\chi^{(2)}$ normalized to its value just before switching off the dc field. It is apparent that the decay dynamics are non-single-exponential and very sensitive to temperature, trademarks of dynamics associated with the α-transition in glass-forming systems.[63]

For measurements at 40 °C, within 200 μs of the removal of the dc field, $\chi^{(2)}_N$ has decreased to a value of 0.84, signifying a 16% decrease in $\chi^{(2)}_N$ as compared to that before removal of the dc field. Much of this decrease is associated with the electric-field-induced third-order effect. In a previous study[48] we have demonstrated that for DR1 the relative contribution of this effect to the overall $\chi^{(2)}$ with the electric field applied is 12 ± 2%, independent of the polymer matrix. With appropriate subtraction of this contribution, the temperature dependence of the decay dynamics associated with the orientation component of $\chi^{(2)}_N$, here designated $\chi^{(2)}_{NO}$, can be determined as shown in Figure 4. Noteworthy is the dramatic difference in the dynamics associated with NLO-chromophore rotational reorientation above and below T_g. At 69 °C, 16 deg above T_g, virtually all of the SHG properties, and thus chromophore orientation, have relaxed away within 1 s of the dc-field removal. However, at 40 °C, 13 deg below T_g, roughly three-quarters of the orientation component of $\chi^{(2)}$ has been retained at 1 s; at 2000 s approximately the same $\chi^{(2)}_{NO}$ is achieved at 40 °C as after only 0.2 s at 69 °C.

As shown by the solid curves in Figure 4, the decay in $\chi^{(2)}_{NO}$ may be modeled by the KWW equation (eq 9). Several points should be noted about these fits. First, when a broad enough range of dynamics is accessed, as in the case where data are taken from 10^{-4} to 10^4 s, it is not possible to model the data by a mono-, bi-, or even triexponential equation, as has often been done in the SHG polymer literature[7,10,12,13,65,66] when measurements have been taken in the absence of short-time (<1 s) data. Instead, only a model which represents a continuous broad distribution of relaxation times can provide an appropriate description of the dynamics in such a system. Secondly, it is necessary that the electric-field-induced third-order effect be subtracted out appropriately before applying the fit to the KWW equation. If this is not done, then any attempt to fit the data (such as the data for $\chi^{(2)}_N$ in Figure 3) by a KWW equation will be in error because those data include the instantaneous decay associated with the third-order effect which is unrelated to the orientation relaxation. Furthermore, this subtraction allows for appropriate normalization of the data, which is not possible by simply normalizing data to a value of 1 at the shortest experimental decay time (often 1 s or longer in other studies[7,8,64,67]). It is evident from the present study that orientation decay has occurred at 40 °C (T_g − 13 °C) on the time scales of 1 ms and less, and by 1 s at least 30% of the orientation component of $\chi^{(2)}$ has decayed away at that temperature.

The temperature dependence of the KWW parameters for decay-mode $\chi^{(2)}_{NO}$ data from 30 to 80 °C is given in Table I. τ is a strong decreasing function of temperature

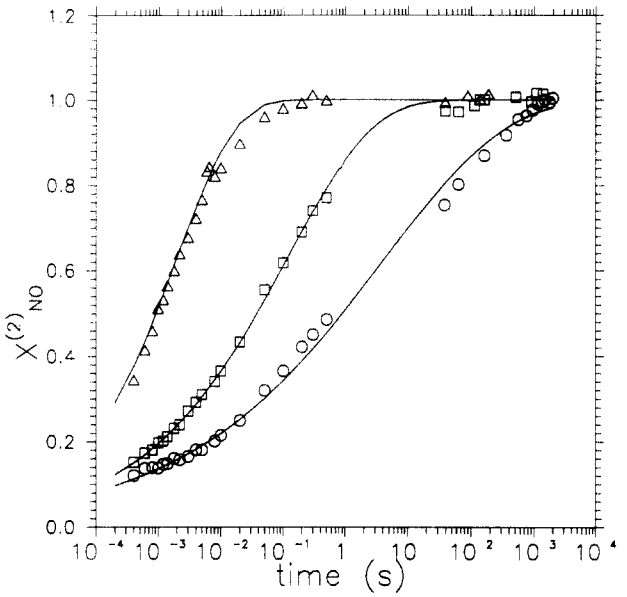

Figure 5. Poling-onset data in PIBMA + 2 wt % DR1 at 51 (○), 63 (□), 80 °C (△). $\chi^{(2)}_{NO}$ is the orientation component of $\chi^{(2)}_N$, the susceptibility normalized with respect to the steady-state value (at the measurement temperature) with the electric field applied. ($\chi^{(2)}_{NO} = [\chi^{(2)}_{zzz}/(0.88\chi^{(2)}_{zzz}(t=\infty)) - 0.12/0.88]$ for the poling-onset data.) The solid curves are fits to the KWW equation.

Table I. Kohlrausch–Williams–Watts Parameters and Average Rotational Time Constants ($\langle\tau\rangle$) as Functions of Temperature from the Decay-Mode Measurements for the PIBMA + DR1 System

temp (°C)	τ (s)	β_w	$\langle\tau\rangle$ (s)
30	1700	0.24	50,000
40	120	0.24	4000
51	11	0.24_7	300
58	0.8	0.29_0	8
63	0.16	0.34_5	0.8
69	0.04	0.35_4	0.2
74	0.007	0.40_8	0.02
80	0.003	0.42_1	0.01

for all temperatures while β_w is a strong increasing function of temperature only above T_g. Average rotational relaxation time constants, $\langle\tau\rangle$, calculated using eq 10, are also given in Table I. $\langle\tau\rangle$ is a very strong decreasing function of temperature in the rubbery state, decreasing by 4 $^1/_2$ orders of magnitude in going from T_g – 2 °C to T_g + 27 °C. The temperature dependence of $\langle\tau\rangle$ is reduced but nevertheless substantial in the glassy state with $\langle\tau\rangle$ decreasing by more than 2 orders of magnitude in going from T_g – 23 °C to T_g – 2 °C.

Very similar conclusions about NLO-chromophore rotational dynamics can be achieved from poling-onset-mode measurements. Figure 5 shows the poling-onset-mode results for the PIBMA + 2 wt % DR1 system at 51, 63, and 80 °C. Here the $\chi^{(2)}_{NO}$ data are equal to the orientation component of $\chi^{(2)}$ normalized to the steady-state value ($t \rightarrow \infty$) with the field applied; the 12% contribution of the electric-field-induced third-order effect[48,49] to $\chi^{(2)}$ has been accounted for in these data. The solid curves in Figure 5 are best fits to the KWW equation (eq 9) with the resulting values of τ, β_w, and $\langle\tau\rangle$ shown in Table II. The values of $\langle\tau\rangle$ are in good agreement with those obtained from the decay-mode measurements. Similar agreement between decay-mode and onset-mode data was observed previously[20] in a PIBMA + 3 wt % DANS (4-(dimethylamino)-4′-nitrostilbene) system. In the case of onset-mode data, it should be noted that results are not reported below T_g. While such measurements are possible, for onset-mode data it may take days to reach and confirm the steady-state value of $\chi^{(2)}$ with the electric field applied. This problem does not arise with the decay-mode data, as the steady-state value of $\chi^{(2)}$ after removal of the dc field is known to be zero.

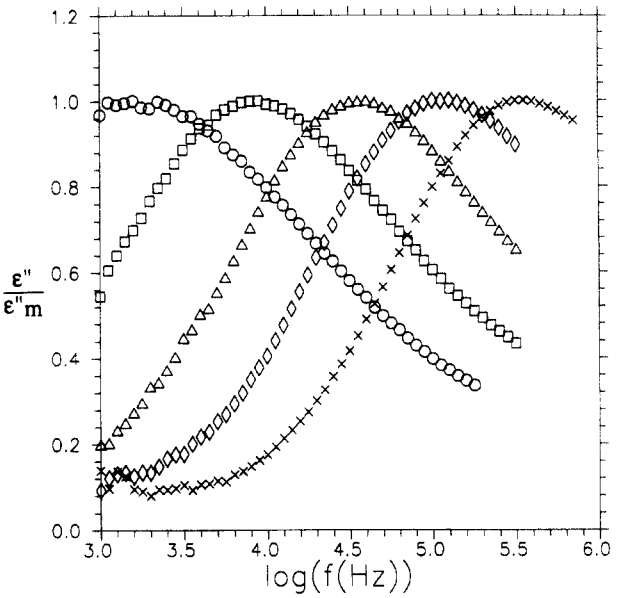

Figure 6. Dielectric relaxation data in PIBMA + 1 wt % DR1 at 103 (○), 113 (□), 124 (△), 134 (◇), and 145 °C (×). ϵ''/ϵ''_m is the dielectric loss normalized by the maximum value at the peak.

Table II. Kohlrausch–Williams–Watts Parameters and Average Rotational Time Constants ($\langle\tau\rangle$) as Functions of Temperature from the Poling-Onset-Mode Measurements for the PIBMA + DR1 System

temp (°C)	τ (s)	β_w	$\langle\tau\rangle$ (s)
51	5	0.22_8	200
63	0.12	0.31_8	0.9
74	0.008	0.39_9	0.03
80	0.002	0.46_4	0.005

Dielectric relaxation measurements have also been done in the rubbery state for a PIBMA + 1 wt % DR1 system. (This system has the same T_g as the systems doped with 2 wt % DR1 used in the SHG studies. Limited comparisons of dielectric relaxation measurements for systems doped with 1 and 2 wt % DR1 reveal nearly identical dielectric relaxation responses.) Figure 6 illustrates the temperature dependence of the dielectric loss component, ϵ'', normalized to the maximum value of ϵ'' at the peak. As expected, the peaks shift to higher frequency with increasing temperature.

Dielectric relaxation data may be analyzed using a variety of models; however, to remain consistent with the analysis of SHG data, the KWW equation (eq 9) has been employed in this case. The complex permittivity, ϵ^*, can be expressed as a one-sided Fourier transform or a pure imaginary Laplace transform of the time derivative of the normalized response function, $\varphi(t)$:[52]

$$\frac{\epsilon^*(\omega) - \epsilon_\infty}{\epsilon_0 - \epsilon_\infty} = \int_0^\infty \left[\frac{-d\varphi(t)}{dt}\right] e^{-i\omega t}\, dt \qquad (13)$$

where $\epsilon^*(\omega) = \epsilon'(\omega) - i\epsilon''(\omega)$, ϵ_0 and ϵ_∞ are the limiting low and high frequency permittivities, respectively, and the response function $\varphi(t)$ is taken to be the KWW function. Theoretically, it is possible to obtain τ and β_w as functions of temperature using eq 13 and the data in Figure 6. However, the data in Figure 6 are not over a broad enough range of frequency to allow unambiguous determination of τ and β_w. An alternative approach is to plot the data

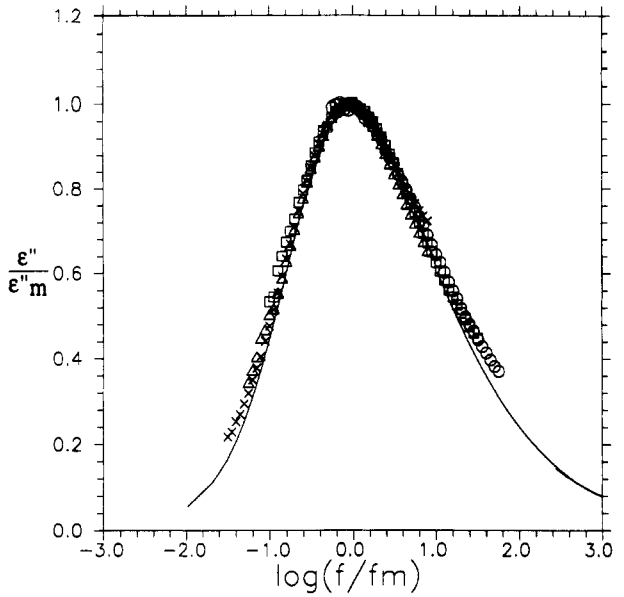

Figure 7. Dielectric relaxation data in PIBMA + 1 wt % DR1 from Figure 6 with the x axis now as $\log(f/f_m)$, where f_m is the frequency at which there is a maximum in ϵ''. The solid curves correspond to fits using the KWW equation with a $\beta_w = 0.5$.

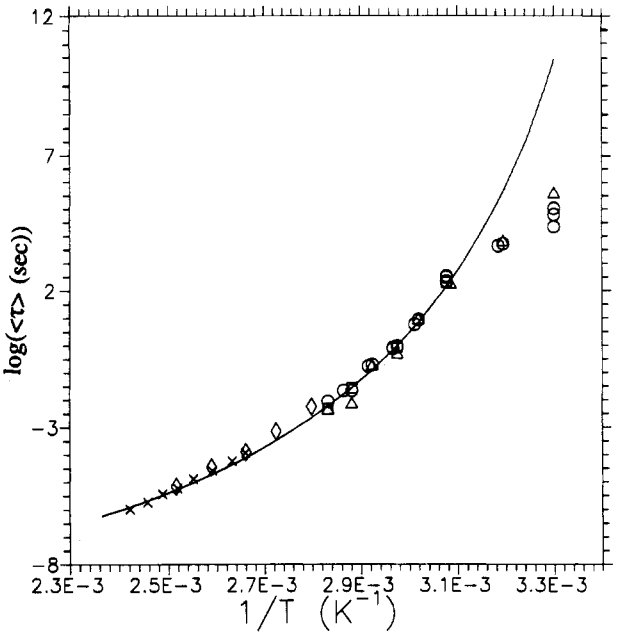

Figure 8. Temperature dependence of the average rotational time constant, $\langle\tau\rangle$, above and below T_g, in PIBMA + 2 wt % DR1 from poling-onset (□) and decay (○) data, PIBMA + 3 wt % DANS (△),[20] PIBMA + 1 wt % DR1 (×) (dielectric relaxation measurement), and PIBMA (◇) (dielectric relaxation measurement from ref 26 using $\beta_w = 0.5$). Solid curve corresponds to a fit using the WLF equation.

in Figure 6 as a function of f/f_m, where f_m is the frequency at which there is a maximum in ϵ''. This approach will be useful if β_w may be approximated as being independent of temperature over the temperatures of interest.

Figure 7 shows that when data taken at different temperatures are plotted as a function of f/f_m, a single master curve with excellent overlap of data results. The solid curve corresponds to a fit using eq 13 with $\beta_w = 0.5$ for all temperatures. In order to determine the KWW parameter τ for each temperature, it is necessary to know the product $(2\pi f_m)\tau$.[68,69] In the case of a single-exponential response function, this product is unity; however, for a response function modeled by the KWW equation, it will be a function of β_w. In the case of $\beta_w = 0.5$, $(2\pi f_m)\tau \approx 0.74$.[68] Given that f_m is a function of temperature, it is possible to determine τ and, using eq 10, $\langle\tau\rangle$.

Figure 8 illustrates the temperature dependence of $\langle\tau\rangle$ obtained from SHG and dielectric relaxation techniques for the PIBMA + DR1 system. Also appearing on the figure are results from the earlier study[20] on the PIBMA + 3 wt % DANS system and values of $\langle\tau\rangle$ obtained from dielectric relaxation data for neat PIBMA by Ishida et al.[26] assuming that $\beta_w = 0.5$. Several important points must be noted from these results. First, very good agreement is observed between the $\langle\tau\rangle$ values obtained by SHG and dielectric relaxation. This indicates that the rotational dynamics of DR1 as measured by SHG are similar to the rotational dynamics of the polar side group of PIBMA as measured by dielectric relaxation. Secondly, the dynamics above T_g clearly cannot be described by an Arrhenius dependence given the strong nonlinearity observed in the dependence of $\langle\tau\rangle$ on $1/T$. Thirdly, the agreement in the DR1 and DANS data indicates that the dynamics of the chromophores are very similar; this is expected given the similar sizes of the chromophores and the identical T_g's of the two systems.

The solid curve in Figure 8 corresponds to a WLF equation (eq 11); from a fit to the data above T_g, $C_1 = 13$, $C_2 = 58°$, and $\langle\tau\rangle_{T_g} \approx 100$ s. While the WLF equation fits the SHG and dielectric relaxation data very well above T_g, there is significant deviation below T_g, where the experimental values of $\langle\tau\rangle$ are far below those predicted by the WLF equation. This is expected, as the WLF equation applies only to the equilibrium rubbery state;[58] the quenched glass has a higher free volume and thus relaxation times smaller than those of the theoretical equilibrium state below T_g. Such effects below T_g have been observed by a variety of studies including dielectric relaxation spectroscopy of poly(vinyl acetate),[70] thermally stimulated discharge measurements in polysulfone,[71] and translational, small-molecule tracer diffusion measurements in a range of polymer matrices.[72] The value of $\langle\tau\rangle_{T_g}$ is in good agreement with values of relaxation times obtained by other techniques in amorphous polymers, including light scattering,[23] NMR,[73], and calorimetric measurements.[63]

It is noteworthy that the deviation in the values of $\langle\tau\rangle$ from the extrapolation of the WLF equation below T_g observed in our studies is in significant conflict with results reported by Goodson and Wang[74,75] who studied a poly(methyl methacrylate) + 3 wt % DANS system ($T_g \approx 85$ °C). They reported that the temperature dependence of τ_2, the slow decay component resulting from a biexponential fit to $\chi^{(2)}$ decay data, was found to follow the Vogel–Tammann–Fulcher (VTF) equation (equivalent to the WLF equation) from $T_g - 30$ °C to $T_g + 20$ °C. Furthermore, the time scales for the decays observed by them at $T_g + 13$ °C (83 s) and $T_g + 20$ °C (27 s) are orders of magnitude beyond the relaxation times observed at comparable temperatures above T_g in our present and previous studies[20] or by other measurements.[23,73]

The reduced but nevertheless significant and apparently Arrhenius temperature dependence of $\langle\tau\rangle$ below T_g has important implications in the design of temporally stable, doped second-order NLO polymers. For example, if technological application mandates no more than a 5–8% loss in $\chi^{(2)}{}_{NO}$ over a 4-year period, then a device could require a $\langle\tau\rangle$ greater than 10^{14} s. (This calculation[76] assumes $\beta_w = 0.24$ as in the case of the glassy PIBMA + 2 wt % DR1 system.) While this large value of $\langle\tau\rangle$ imposes severe device requirements, it may be possible to predict the conditions necessary to achieve this long-time per-

formance using the approaches described in this study. For example, if studies were to reveal an Arrhenius temperature dependence of $\langle\tau\rangle$ in the glassy state of the polymer + dye system under consideration, with β_w constant over a broad range of T, then it should be possible to predict the glassy state temperature meeting the required objective for device application. Although the exact temperature dependence of $\langle\tau\rangle$ in the glassy state has yet to be determined, it is clear from the present studies that technological applications would require the use temperature to be far below T_g (possibly $<T_g - 150$ °C) for the case of thermally quenched, doped polymer systems.

The excellent agreement between SHG data (reflective of chromophore dynamics) and dielectric relaxation results (reflective of polymer dynamics) above T_g as well as the deviation in SHG results from WLF behavior below T_g indicate that the rotational dynamics of the nonlinear optical chromophore DR1 are directly coupled to polymer dynamics. In order to reach this conclusion definitively, it was necessary that both very fast ($<10^{-3}$ s) and very slow ($>10^3$ s) dynamics be accessed and that the contribution of the electric-field-induced third-order effect of $\chi^{(2)}$ be adequately taken into account. In the absence of such information, several other pictures were recently proposed in order to explain the NLO-chromophore orientation mechanism below T_g. Boyd et al.[18] proposed that NLO chromophores in glassy polymers are surrounded by excess free volume and that the dipoles may be constrained within the voids. Kuzyk et al.[19] proposed that an additional elastic force is present below T_g in glassy polymers which constrains NLO chromophore mobility. Given the data available to those researchers, the pictures developed were consistent with their results. However, when a more complete experimental analysis is achieved, it is seen that it is unnecessary to invoke these very specific models and instead that the general picture related to polymer-segment and -chain dynamics is sufficient to explain the behavior.

The dielectric relaxation data for PIBMA are indicative of the α-relaxation, i.e., the cooperative segmental mobility of a small number of repeat units in the chain backbone of the polymer;[29] no β-transition is apparent in the dielectric spectrum[77] for PIBMA. (This in turn implies that the onset of mobility for the large polar side group in PIBMA is coincident with segmental mobility of the PIBMA backbone.) Thus, one may conclude from these results that both DR1 and DANS rotational, reorientation dynamics are coupled to the motions associated with the α-transition in PIBMA. Similar indications have been reached for other NLO chromophore–polymer SHG studies,[15,17] but none of the previous studies has quantitatively shown the connection as demonstrated in the present study. Other experimental techniques have also rendered similar conclusions regarding the coupling of dopant and polymer rotational dynamics. For example fluorescence anisotropy decay studies by Hyde and Ediger[38] have indicated that the rotational motion of anthracene in polyisoprene is sensitive to the α- and not the β-motion. However, polyisoprene exhibits only a weak β-relaxation. Given that as well as the fact that PIBMA studied here exhibits no β-relaxation, it is important to study NLO-chromophore rotational dynamics in a polymer exhibiting both strong α- and β-relaxations in order to conclude convincingly that for DR1 the rotational dynamics are coupled to α- and not to β-relaxations. Such a study can be achieved with PEMA.

(C) Temperature Dependence in PEMA. Figure 9 shows the decay-mode results for $\chi^{(2)}_{NO}$ in a PEMA + 2 wt % DR1 system at 30, 49, and 69 °C. (These data were obtained from decays of SHG intensities in a manner similar to that used for the data given in Figure 4.) The solid curves correspond to fits using the KWW equation (eq 9). Similar trends are observed in the decay dynamics as for the PIBMA + DR1 system in that they cannot be described by mono-, bi-, or triexponential decays and that they are a strong function of temperature near T_g. Decay-mode data were obtained for the PEMA system from 30 to 69 °C. Rotational dynamics of DR1 were studied above 69 °C using onset-mode measurements.

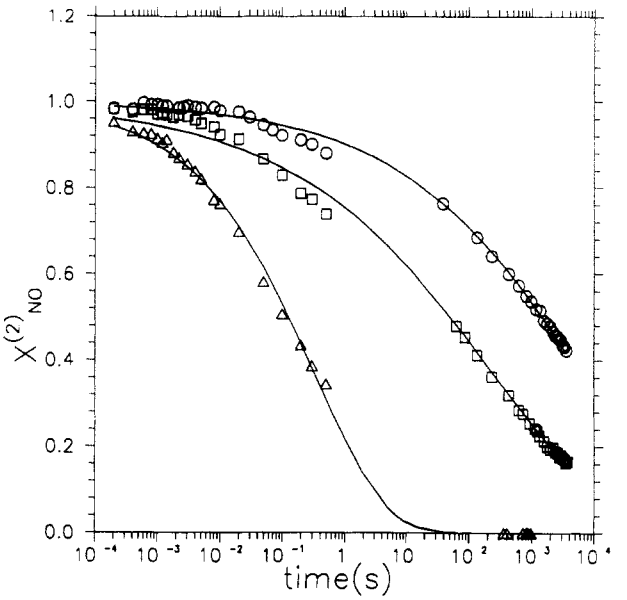

Figure 9. Decay data in PEMA + 2 wt % DR1 at 30 (○), 49 (□), and 69 °C (△). $\chi^{(2)}_{NO}$ is the orientation component of the macroscopic susceptibility $[\chi^{(2)}_{zzz}/(0.88\chi^{(2)}_{zzz}(t=0))]$. The solid curves are fits to the KWW equation.

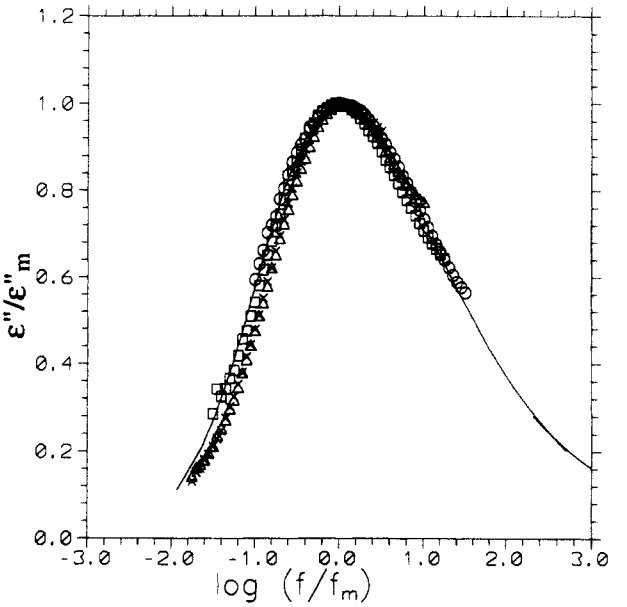

Figure 10. Dielectric relaxation data in PEMA + 2 wt % DR1 at 107 (○), 117 (△), 126 (□), and 135 °C (×). The x axis is log-(f/f_m), where f_m is the frequency at which there is a maximum in dielectric loss, ϵ'' (ϵ''_m). The solid curves correspond to fits using the KWW equation with a $\beta_w = 0.4$.

Figure 10 shows dielectric relaxation data for PEMA + 2 wt % DR1 as a function of temperature from 107 to 135 °C with the data plotted in a manner similar to Figure 7. There is excellent overlap of the data onto a single master curve, indicating that β_w is independent of temperature for the temperatures studied. The solid curve in Figure

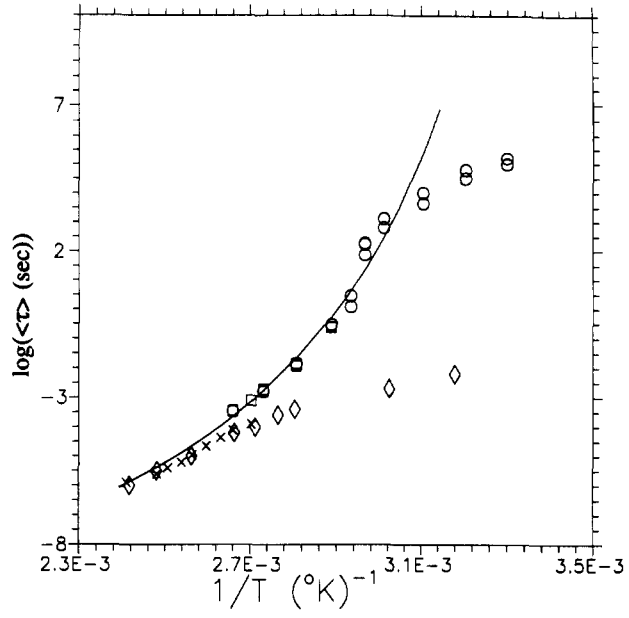

Figure 11. Temperature dependence of the average rotational time constant, $\langle\tau\rangle$, above and below T_g, in PEMA + 2 wt % DR1 from the poling-onset (□) and decay (○) data, PEMA + 2 wt % DR1 (×) (dielectric relaxation measurement), and PEMA (◇) (dielectric relaxation measurement from ref 26 using $\beta_w = 0.4$). Solid curve corresponds to a fit using the WLF equation.

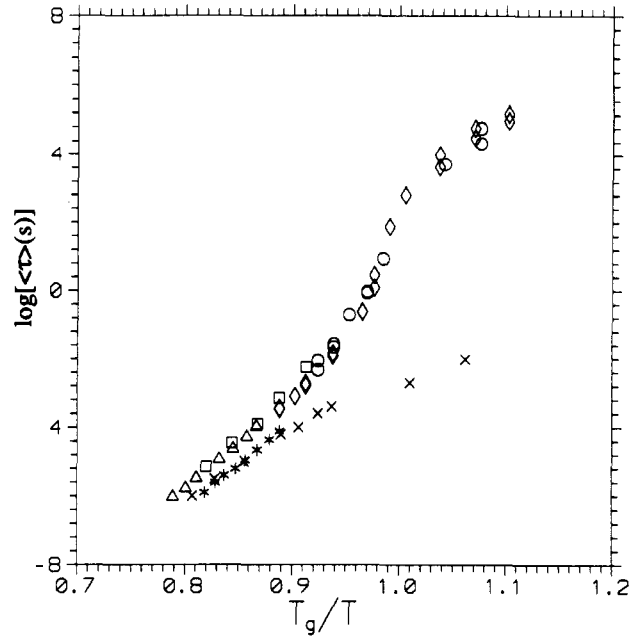

Figure 12. Values of $\langle\tau\rangle$ from both SHG and dielectric relaxation measurements (Figures 8 and 11) scaled using the reduced variable T_g/T: PIBMA + DR1 (○) (SHG); PIBMA (□) (dielectric relaxation from ref 26); PIBMA + 1 wt % DR1 (△) (dielectric relaxation); PEMA + 2 wt % DR1 (◇) (SHG); PEMA + 2 wt % DR1 (*) (dielectric relaxation); PEMA (×) (dielectric relaxation from ref 26).

10 corresponds to a fit using eq 13 and the KWW equation (eq 9) as the response function with $\beta_w = 0.4$. It is interesting to note that Patterson et al.[22] obtained $\beta_w = 0.4$ at 120 °C in PEMA from photon correlation spectroscopy.

Using the results of the analyses of data in Figures 9 and 10, the temperature dependence of $\langle\tau\rangle$ from SHG and dielectric relaxation measurements may be determined, as shown in Figure 11. Also shown in Figure 11 are results from dielectric relaxation studies by Ishida and Yamafuji,[26] plotted assuming that $\beta_w = 0.4$. Similar to the PIBMA + DR1 system (Figure 8), above T_g a strong, non-Arrhenius temperature dependence of the SHG data is observed. However, unlike the results for PIBMA + DR1, there is not a good correspondence between the SHG and dielectric data for $T \leq 1.15$–$1.17T_g$; we believe the dielectric data at these temperatures are associated with the β-transition.[78] In polymers exhibiting both α- and β-relaxations, such as PEMA, it is known that at temperatures somewhat above T_g the β-relaxation merges into the α-relaxation. It has been shown recently by Rossler[79] that in supercooled, small molecule liquids there is a merger of the β-relaxation with the α-relaxation near $1.2T_g$. Similar results were also obtained in polystyrene[73] where the α- and β-relaxations merge around 1.1–$1.2T_g$. Our current results in PEMA support the experimental observations by Rossler[79] and Pschorn et al.[73] It is also noteworthy that the $\langle\tau\rangle$ values obtained for homopolymer PEMA from photon correlation spectroscopy by Patterson et al.[22] are in good agreement with the $\langle\tau\rangle$ values in Figure 11 obtained from SHG measurements.

The solid curve in Figure 11 represents a fit to a WLF equation (eq 11 with $C_1 = 14$, $C_2 = 62°$, and $\langle\tau\rangle_{T_g} \approx 100$ s) for the SHG data above T_g and the dielectric relaxation data at $T \geq 1.2T_g$. (At high temperatures, the dielectric relaxation data are indicative of α-transition dynamics.) The agreement between the SHG data and the high temperature dielectric data in fitting a single WLF equation and the significant disagreement between SHG data and dielectric data for $T < 1.15$–$1.17T_g$ (where dielectric data are indicative of β-transition dynamics) strongly indicate that the rotational dynamics of DR1 in PEMA are coupled to the α- and not the β-relaxation dynamics.

(D) Scaling with the Reduced Variable T_g/T. While the major conclusion of this study is that the rotational dynamics of NLO chromophores such as DR1 and DANS are coupled to α-transition dynamics when they are doped in polymers such as PIBMA and PEMA, other implications of this work deserve notice. The $\langle\tau\rangle$ results from Figures 8 and 11 indicative of the α-relaxation process can be shown to fit well to a single master curve by scaling the data using the reduced variable T_g/T, implying similarity in the cooperativity of the α-relaxation in PIBMA and PEMA. This scaling has been used recently by Angell[63] to compare macroscopic viscosity for glass-forming systems (in his approach for classifying "fragile" and "strong" glass formers) and by Roland and Ngai[80] to compare α-transition dynamics for various molecular weights of polystyrene. Rossler[79] has also used a similar scaling approach employing T_r/T where T_r is correlated with T_g. Figure 12 combines the PIBMA and PEMA data from Figures 8 and 11 onto a single plot employing T_g/T as the abscissa. The substantial overlap of data sensitive to the α-relaxation for these two systems suggests similarity in the cooperativity of the α-transition in these two polymers and that these polymers are closer to the strong glass formers in Angell's classification scheme.[63] Further, these results suggest that this scaling approach for similar types of polymers may be very valuable in predicting α-transition-based behavior without performing experiments. The generality (or lack thereof) of this approach across polymer types is the subject of current study; SHG results in polystyrene, structurally very different from methacrylate-based polymers, will be compared to those in PIBMA and PEMA in the near future.[81]

Summary

Employing a delay-trigger approach as well as conventional SHG measurements allowing access to fast (10^{-4} s)

as well as very slow dynamics, this study has demonstrated quantitatively that the transient dynamics of $\chi^{(2)}$, e.g. the temporal decay of $\chi^{(2)}$ upon removal of the applied dc field, are associated with two effects. The smaller effect is due to the electric-field-induced third-order effect[48] which for all practical purposes is instantaneous. The larger effect is due to the orientation component of $\chi^{(2)}$. In agreement with predictions by Wu,[59] $\chi^{(2)}_{zzz}$ and $\chi^{(2)}_{zxx}$ dynamics were shown to be equivalent, implying that the transient dynamics associated with the orientation component of $\chi^{(2)}$ are sensitive to $\langle \cos\theta \rangle$, where θ is the angle between the direction vector of the applied dc field and that of the NLO-chromophore dipole moment. Furthermore, $\chi^{(2)}_{zzz}/\chi^{(2)}_{zxx} = 3.0$, supporting the use of Boltzmann statistics in describing the distribution of NLO-chromophore orientation in rubbery and glassy polymers.

The time dependence of both the onset- and decay-mode orientation components of $\chi^{(2)}$ can be represented by the KWW equation. The KWW parameters determined from these fits reveal different temperature dependencies near T_g, with τ being a strong function of T for $T < T_g + 30$ °C while β_w is a strong function of T from T_g to $T_g + 30$ °C but nearly independent of T below T_g. Using the calculated τ and β_w parameters, average rotational, reorientation relaxation times $\langle \tau \rangle$ are easily calculable. In agreement with predictions of the WLF equation, the temperature dependence of $\langle \tau \rangle$ is very strong near T_g; below T_g, it is weaker but nevertheless substantial. In PIBMA and PEMA, $\langle \tau \rangle_{T_g}$ is about 2 min, in reasonable agreement with the time scale of enthalpy relaxation (considered sensitive to all conformational relaxations) normally associated with T_g in calorimetric measurements.[63]

Comparison of SHG results of DR1 and DANS dopant reorientation in PIBMA and PEMA to dielectric relaxation results (sensitive to polymer dynamics and also associated with $\langle \cos\theta \rangle$[60]) revealed that the NLO dopant rotational dynamics are coupled to the α-relaxation associated with the glass transition in these polymers. Reasonable fits above T_g of SHG and α-relaxation-sensitive dielectric relaxation data to the WLF equation also support this conclusion. As a result of this coupling and the very broad dynamic range afforded by this technique, SHG may become an important new tool in studying α-relaxation dynamics under circumstances not easily accessed by other techniques. By scaling $\langle \tau \rangle$ data with the reduced parameter T_g/T, a substantial similarity of the cooperativity of the α-transition in PIBMA and PEMA was revealed. For second-order NLO application of linear thermoplastics to be achieved, the coupling of the chromophore and polymer dynamics demonstrates the requirement to understand the underlying polymer physics responsible for the temporal decay of SHG in poled polymers. Extensions of these studies to the effects of chromophore size and concentration and covalent attachment[82] of the chromophore to the polymer are underway.

Acknowledgment. We gratefully acknowledge the Materials Research Center at Northwestern University funded by the National Science Foundation and the receipt of a Terminal Year Cabell Fellowship (A.D.) and NSF-PYI award (J.M.T.) for supporting this work. We also thank Professor T. O. Mason (Materials Science & Engineering, Northwestern University) for use of the dielectric spectrometer, Mr. Bruce Christensen (Materials Science & Engineering, Northwestern University) for helpful discussions and instructions regarding its use, and Mr. Bob Lloyd and Mr. Peter Weiss (Chemistry Electronics Shop, Northwestern University) for their help in building the electronics for our delay-trigger method.

References and Notes

(1) Meredith, G. R.; VanDusen, J. G.; Williams, D. J. *Macromolecules* **1982**, *15*, 1385.
(2) Williams, D. J. *Angew. Chem., Int. Ed. Engl.* **1984**, *23*, 690.
(3) Willand, C. S.; Williams, D. J. *Ber. Bunsen-Ges. Phys. Chem.* **1987**, *91*, 1304.
(4) Herminghaus, S.; Smith, B. A.; Swalen, J. D. *J. Opt. Soc. Am. B* **1991**, *8*, 2311.
(5) Singer, K. D.; Kuzyk, M. G.; Holland, W. R.; Sohn, J. E.; Lalama, S. J.; Cormizzoli, R. B.; Katz, H. E.; Schilling, M. J. *Appl. Phys. Lett.* **1988**, *53*, 1800.
(6) Van Eck, T. E.; Ticknor, A. J.; Lytel, R. S.; Lipscomb, G. F. *Appl. Phys. Lett.* **1991**, *58*, 1588.
(7) (a) Hampsch, H. L.; Yang, J.; Wong, G. K.; Torkelson, J. M. *Macromolecules* **1988**, *21*, 526. (b) Hampsch, H. L.; Yang, J.; Wong, G. K.; Torkelson, J. M. *Macromolecules* **1990**, *23*, 3640.
(8) Singer, K. D.; King, L. A. *J. Appl. Phys.* **1991**, *70*, 3251.
(9) Ye, C.; Marks, T. J.; Yang, J.; Wong, G. K. *Macromolecules* **1987**, *20*, 2324.
(10) Hubbard, M. A.; Marks, T. J.; Yang, J.; Wong, G. K. *Chem. Mater.* **1989**, *1*, 167.
(11) Eich, M.; Reck, B.; Yoon, D. Y.; Wilson, C. G.; Bjorklund, G. C. *J. Appl. Phys.* **1989**, *66*, 3241.
(12) Eich, M.; Sen, A.; Looser, G. C.; Bjorklund, G. C.; Swalen, J. D.; Tweig, R.; Yoon, D. Y. *J. Appl. Phys.* **1989**, *66*, 1989.
(13) Ye, C.; Minami, N.; Marks, T. J.; Yang, J.; Wong, G. K. In *Nonlinear Optical Effects in Organic Polymers*; Messier, J., Ed.; Kluwer Academic Publishers: Dordrecht, The Netherlands, 1989; p 173.
(14) Amano, M.; Kaino, T. *J. Appl. Phys.* **1990**, *68*, 6024.
(15) Eich, M.; Looser, H.; Yoon, D. Y.; Twieg, R.; Bjorklund, G.; Baumert, J. C. *J. Opt. Soc. Am. B* **1989**, *6*, 1590.
(16) Kohler, W.; Robello, D. R.; Willand, C. S.; Williams, D. J. *Macromolecules* **1991**, *24*, 4589.
(17) Kohler, W.; Robello, D. R.; Dao, P. T.; Willand, C. S.; Williams, D. J. *J. Chem. Phys.* **1990**, *93*, 9157.
(18) Boyd, G. T.; Francis, C. V.; Trend, J. E.; Ender, D. A. *J. Opt. Soc. Am. B* **1991**, *8*, 887.
(19) Kuzyk, M. G.; Moore, R. C.; King, L. A. *J. Opt. Soc. Am. B* **1990**, *7*, 64.
(20) Dhinojwala, A.; Wong, G. K.; Torkelson, J. M. *Macromolecules* **1992**, *25*, 7395.
(21) Levine, B. F.; Bethea, C. G. *J. Chem. Phys.* **1976**, *65*, 1989.
(22) Patterson, G. D.; Stevens, J. R.; Lindsey, C. P. *J. Macromol. Sci.—Phys.* **1980**, *18*, 641.
(23) Patterson, G. D.; Lindsey, C. P.; Stevens, J. R. *J. Chem. Phys.* **1979**, *70*, 643.
(24) Lee, H.; Jamieson, A. M.; Simha, R. *Colloid Polym. Sci.* **1980**, *258*, 545.
(25) McCrum, N. G.; Read, B. E.; Williams, G. *Anelastic and Dielectric Effects in Polymeric Solids*; Dover Publications, Inc.: New York, 1991.
(26) Ishida, Y.; Yamafuji, K. *Kolloid-Z.* **1961**, *177*, 97.
(27) Adachi, K.; Kotaka, T. *Macromolecules* **1985**, *18*, 466.
(28) Boese, D.; Momper, B.; Meier, G.; Kremer, F.; Hagenah, J.-U.; Fisher, E. W. *Macromolecules* **1989**, *22*, 4416.
(29) Ferry, J. D. *Viscoelastic Properties of Polymers*; J. Wiley: London, 1980.
(30) Heijboer, J. In *Static and Dynamic Properties of the Polymeric Solid State*; Pethrick, R. A., Richards, R. W., Ed.; D. Reidel Publishing Co.: Holland, 1982; pp 197–211.
(31) Spiess, H. W. *Colloid Polym. Sci.* **1983**, *261*, 193.
(32) Rossler, E.; Sillescu, H.; Spiess, H. W. *Polymer* **1985**, *26*, 203.
(33) Veissier, V.; Viovy, J.-L.; Monnerie, L. *Polymer* **1989**, *30*, 1262.
(34) (a) Ediger, M. D. *Annu. Rev. Phys. Chem.* **1991**, *42*, 225. (b) Hyde, P. D.; Ediger, M. D.; Kitano, T.; Koichi, I. *Macromolecules* **1989**, *22*, 2253.
(35) Sasaki, T.; Arisawa, H.; Yamamoto, M. *Polym. J.* **1991**, *23*, 103.
(36) Bokobza, L. *Prog. Polym. Sci.* **1990**, *15*, 337.
(37) Freeman, B. D.; Bokobza, L.; Sergot, P.; Monnerie, L.; De Schryver, F. C. *Macromolecules* **1990**, *23*, 2566.
(38) Hyde, P. D.; Ediger, M. D. *J. Chem. Phys.* **1990**, *92*, 1036.
(39) Cicerone, M. T.; Ediger, M. D. *J. Chem. Phys.* **1992**, *97*, 2156.
(40) Jones, P.; Jones, W. J.; Williams, G. *J. Chem. Soc., Faraday Trans.* **1990**, *86*, 1013.
(41) Prasad, P. N.; Williams, D. J. *Introduction to Nonlinear Optical Effects in Molecules and Polymers*; John Wiley & Sons, Inc.: New York, 1991.
(42) Singer, K. D.; Kuzyk, M. G.; Sohn, J. E. *J. Opt. Soc. Am. B* **1987**, *4*, 968.

(43) Boyd, R. W. *Nonlinear Optics*; Academic Press Inc.: San Diego, 1992.
(44) Shen, Y. R. *The Principles of Nonlinear Optics*; John Wiley: New York, 1984.
(45) Singer, K. D.; Sohn, J. E.; King, L. A.; Gordon, H. M.; Katz, H. E.; Dirk, C. W. *J. Opt. Soc. Am. B* **1989**, *6*, 1339.
(46) Lalama, S. J.; Garito, A. F. *Phys. Rev. A* **1979**, *20*, 1179.
(47) Levine, B. F.; Bethea, C. G. *J. Chem. Phys.* **1975**, *63*, 2666.
(48) Dhinojwala, A.; Wong, G. K.; Torkelson, J. M. *J. Opt. Soc. Am. B*, in press.
(49) As γ is a characteristic of the chromophore and has nothing to do with the polymer or its associated dynamics, its contribution to $\chi^{(2)}_N$ was determined by decay measurements at 30 °C in two other polymers, PEMA and poly(methyl methacrylate), besides PIBMA. It is especially noteworthy that, in these higher T_g polymers, $\chi^{(2)}_N \approx 0.88$ over the time range 2×10^{-4} to 0.5 s, making it clear that γ accounts for 12% of the overall steady state $\chi^{(2)}$ with the electric field applied.
(50) (a) Kohlrausch, R. *Ann. Phys. (Leipzig)* **1847**, *12*, 393. (b) Williams, G.; Watts, D. C. *Trans. Faraday Soc.* **1970**, *66*, 80.
(51) The KWW equation can also originate from the coupling model proposed by Ngai et al. (Ngai, K. L.; Rajgopal, A. K.; Teitler, S. *J. Chem. Phys.* **1988**, *88*, 5086.)
(52) Williams, G.; Watts, D. C. In *NMR Basic Principles and Progress*; Diehl, P., et al., Eds.; Springer-Verlag: New York, 1970, Vol. 4.
(53) (a) Berens, A. R.; Hodge, I. M. *Macromolecules* **1982**, *15*, 756. (b) Hodge, I. M.; Havard, G. S. *Macromolecules* **1983**, *16*, 371.
(54) Matsuoka, S.; Williams, G.; Johnson, G. E.; Anderson, E. W.; Furukawa, T. *Macromolecules* **1985**, *18*, 2652.
(55) Rossler, E. *J. Chem. Phys.* **1990**, *92*, 3725.
(56) Matsuoka, S.; Quan, X. *Macromolecules* **1991**, *24*, 2770.
(57) Kremer, F.; Boese, D.; Meier, G.; Fischer, E. W. *Prog. Colloid Polym. Sci.* **1989**, *80*, 129.
(58) Williams, M. L.; Landel, R. F.; Ferry, J. D. *J. Am. Chem. Soc.* **1955**, *77*, 3701.
(59) Wu, J. W. *J. Opt. Soc. Am. B* **1991**, *8*, 142.
(60) Debye, P. *Polar Molecules*; Chemical Catolog. Co.: New York, 1929; p 27.
(61) It is crucial that a study of the type presented here be done using "contact" or electrode poling rather than corona poling. Corona poling[7b] introduces many complicated issues related in part to a time-dependent retention of surface charge in the polymer that may often mask the effects of polymer physics associated with NLO chromophore rotational dynamics. Even in the case of electrode poling, the particular substrate and electrode materials may be important. For example, if one uses ordinary glass substrate instead of quartz, then additional charge injection effects (Yitzchaik, S.; Berkovic, G.; Krongauz, V. *Opt. Lett.* **1990**, *15*, 1120) may be seen. It is also important to note that using harsh poling conditions such as high temperature and high voltages leads to other extraneous effects which could affect the rotational dynamics of the chromophores.
(62) We have recently reduced the fall times of the high voltage to less than 2 μs, which allows us to monitor the transient dynamics on time scales as small as 5 μs.
(63) Angell, C. A. *J. Non-Cryst. Solids* **1991**, *131–133*, 13.
(64) Stahelin, M.; Walsh, C. A.; Burland, D. M.; Miller, R. D.; Tweig, R. J.; Volksen, W. *J. Appl. Phys.* **1993**, *73*, 8471.
(65) Park, J.; Marks, T. J.; Yang, J.; Wong, G. K. *Chem. Mater.* **1990**, *2*, 229.
(66) Man, H.-T.; Yoon, H. N. *Adv. Mater.* **1992**, *4*, 159.
(67) Stahelin, M.; Burland, D. M.; Ebert, M.; Miller, R. D.; Smith, B. A.; Twieg, R. J.; Volksen, W.; Walsh, C. A. *Appl. Phys. Lett.* **1992**, *61*, 1627.
(68) Lindsey, C. P.; Patterson, G. D. *J. Chem. Phys.* **1980**, *73*, 3348.
(69) Patterson, G. D. In *Light Scattering from Polymer*; Cantow, H.-J., et al., Ed.; Springer-Verlag: Berlin Heidelberg: New York, 1983.
(70) Schlosser, E.; Schonhals, A. *Polymer* **1991**, *32*, 2135.
(71) Colmenero, J. *J. Non-Cryst. Solids* **1991**, *131*–133, 860.
(72) Ehlich, D.; Sillescu, H. *Macromolecules* **1990**, *23*, 1600.
(73) Pschorn, U.; Rossler, E.; Kaufmann, S.; Sillescu, H.; Speiss, H. W. *Macromolecules* **1991**, *24*, 398.
(74) Goodson, T., III; Wang, C. H. *Macromolecules* **1993**, *26*, 1837.
(75) Goodson and Wang[74] also noted that their investigation disagreed with data we reported earlier in a preprint (Dhinojwala, A.; Wong, G. K.; Torkelson, J. M. *Polym. Prepr. (Am. Chem. Soc., Div. Polym. Chem.)* **1991**, *32*, 100.). For the data reported in that preprint (Figure 1), poling of the samples was limited to 1.5 min both above and below T_g. Since the samples poled below T_g never reached a steady-state value of $\chi^{(2)}$ prior to removal of the dc field, the decay of $\chi^{(2)}$ upon removal of the electric field resulted in a loss of SHG signal within 1.5 min. Thus the interpretation by Goodson and Wang that we had missed the slow decay due to temperature inhomogeneity or limited sensitivity of the detection scheme is not correct since we had never poled long enough for the data reported in that preprint (Figure 1) to see any slow component below T_g. We regret any misconceptions due to the wording used in the preprint that may have arisen regarding our work.
(76) With $\beta_w = 0.24$, $t = 1.2 \times 10^8$ s, and $\exp(-(t/\tau)^{\beta_w}) \approx 0.92$ we obtain $\tau \approx 3 \times 10^{12}$ s, which corresponds to $\langle\tau\rangle \approx 10^{14}$ s.
(77) Data from this study as well as ref 26 support this conclusion.
(78) The merger of α- and β-relaxations in PEMA is observed in Figure 4 of ref 26 where the α-peak merges with the β-peak around 117.3–130.3 °C. The merger of the α- and β-relaxations may also be estimated for our DR1-doped PEMA from the change in the slope of the dielectric relaxation data in Figure 11, which occurs around $1.15–1.17T_g$ (111–119 °C).
(79) Rossler, E. *J. Non-Cryst. Solids* **1991**, *131–133*, 242.
(80) Roland, C. M.; Ngai, K. L. *Macromolecules* **1992**, *25*, 5765.
(81) Dhinojwala, A.; Wong, G. K.; Torkelson, J. M. *J. Chem. Phys.*, submitted for publication.
(82) Dhinojwala, A.; Hooker, J. C.; Torkelson, J. M. *J. Non-Cryst. Solids*, submitted for publication.